RSC Advances

ROYAL SOCIETY OF CHEMISTRY

www.rsc.org/advances

Journal Name

ARTICLE

Enhanced amoxicillin treatment using electro-peroxone process: key factors and degradation mechanism

Received 00th January 20xx,
Accepted 00th January 20xx

DOI: 10.1039/x0xx00000x

www.rsc.org/

Wanqian Guo*, Qu-Li Wu, Xian-Jiao Zhou, Hai-Ou Cao, Juan-Shan Du, Ren-Li Yin, Nan-Qi Ren[c]

Amoxicillin (AMO) degradation was investigated using electrolysis, ozonation, and electro-peroxone (E-peroxone) process. E-peroxone process was found to be the most effective for AMO degradation. 67.8% total organic carbon (TOC) mineralization was obtained after 60 min by E-peroxone process. In comparison, only 47.3% and 3.1% TOC mineralization were obtained using individual ozonation and electrolysis process, respectively. It was found that hydroxyl radical production and O3 utilization were both enhanced in E-peroxone process. The effect of pH on E-peroxone process was investigated, and the highest AMO removal rate was obtained at pH= 9, indicating pH control was crucial in E-peroxone process. In addition, more oxidation typical intermediates were identified in E-peroxone process than ozonation process using UPLC-MS/MS. Different pathways of AMO degradation were proposed, involving the hydroxylation of the benzoic ring and N, the four-membered β-lactamic ring opening, the oxidation of S, and other bond cleavage reactions. All these results above indicated that the introduction of electrolysis in ozonation has enhanced AMO cleavage and hence its degradation.

Introduction

Antibiotics are widely used for curing human and veterinary diseases, as well as feed additives for livestock growth. Due to the potential adverse effects on aquatic ecology [1] and human health [2-4], the present of antibiotics in aquatic environments received special concern. Recent studies reported that the antibiotics concentration in aquatic environments ranged from ng•L^{-1} to μg•L^{-1} in USA, Canada, Germany and China [5-8]. Amoxicillin (AMO), a broad-spectrum amino penicillin antibiotic, which was widely used as a kind of veterinary antibiotic in aquaculture, animal husbandry and also human medicine. Terribly, AMO has been found in a certain amount in water environment that threats human health. It was reported the AMO concentration was up to about 0.6 μg•L^{-1} in British rivers [9], as well as 13 ng•L^{-1} in a municipal sewage treatment plant in Italy [10]. Due to the antibacterial nature and its toxicity, AMO shows resistance to conventional biological water treatment methods. Thus, it is necessary to develop efficient treatment techniques to prevent AMO entering into aquatic environment.

Ozonation was proposed to be a suitable process for antibiotics treatment (removal), due to the strong oxidation ability of ozone (E_0=2.07 V). Ozone molecular was proved to have a high selectivity in attacking conjugated double bonds (e.g., N=N, C=N, and C=C), aromatic bonds or nitrogen, phosphorous, oxygen or sulphur atoms[11], since it only selectively reacted with nucleophilic molecules[12]. Previous investigations have already demonstrated that ozone is capable of attacking those present β-lactams antibiotics (including AMO) in water. Although high removal rates were achieved, the degree of mineralization was low (<20%), even undergoing for a long treatment time [13, 14]. Due to the low mineralization degree, biodegradability enhancement (increment of BOD5/COD ratio) was slight after the ozonation treatment [15].

To improve the mineralization efficiency, combined ozone processes were used in antibiotic wastewater treatment, particularly combined O_3 and electrolysis process (the so-called electro-peroxone process). The main mechanism of electro-peroxone is that O_3 can react with H_2O_2 which is generated by the electrical process in situ, to form hydroxyl radical (•OH) [16, 17], which can improve the mineralization efficiencies of pollutants than ozonation remarkably [18]. In addition, electro-peroxone process produced none secondary pollutants, only leaving H_2O and O_2 as by-products[19, 20]. Therefore, electro-peroxone process was considered as an effective and environmental-friendly advanced oxidation technology for wastewater treatment [18, 21]. Meanwhile, electro-peroxone has some advantages over peroxone process such as that the addition of small amounts of hydrogen peroxide increased the removal efficiency (up to 15%) and the effluents biodegradability, the biotoxicity was not removed completely [22, 23]. However, H_2O_2 is unsafe to transport, store and handle, due to its high reactivity. High concentrations of H_2O_2 addition would decrease the process efficiency, since excess H_2O_2 may act as a free radical scavenger. Electro-peroxone process would use the H_2O_2 more economically and efficiently than other individual process. Particularly, E-peroxone processes have already been applied to the dye wastewater treatment and landfill leachate treatment successfully [24,25]. Despite so many advantages, the AMO wastewater treatment using E-peroxone has not been reported yet.

This study focused on the performance of the E-peroxone process by using activated carbon fiber (ACF) cathode for antibiotic

[a] State Key Laboratory of Urban Water Resource and Environment, Harbin Institute of Technology
[b] 73 Huanghe Road, Harbin, Heilongjiang, 150090, P. R. China

removal, and chose AMO as the model compound. The main objective of this work was to examine the feasibility of AMO treatment using E- peroxone. The operation and AMO degradation pathways were also discussed.

Experimental

Chemicals and reagents

AMO ($C_{16}H_{18}N_3NaO_5S$, analytical reagent, 99.0%) was purchased from TCI and used as received without further purification. Hydroxyterephthalic acid (HTA, 97%) was purchased from Sigma-Aldrich. Terephthalic acid (TA, > 99%) was purchased from Alfa Aesar. Other chemicals (e.g. Na_2SO_4, NaOH, and K_2HPO_4, H_3PO_4 and KH_2PO_4,) were analytical grade and purchased from Tianjin chemical Works Co., China. All solutions were prepared using deionized water.

Ozonation, electrolysis, and E-peroxone process of AMO

AMO solutions were buffered by the addition of K_2HPO_4, H_3PO_4 and KH_2PO_4. Oxidation experiments were carried out in a 1.0L reactor with a continuous supply of O_3. Ozonation, electrolysis, and E-peroxone process of 1.0L AMO (initial concentration of 100 mg•L-1) were carried out in an undivided acrylic cube reactor designed originally. For ozonation process, ozone was produced from pure O_2 gas (99.9%) using an ozone generator with gaseous flow meter (DHX-SS-1G, Jiujiu ozone, Harbin, China). The ozone effluent was placed on the bottom of the reactor, using a fine bubble diffuser at a constant flow rate of 0.4 L•min^{-1} unless otherwise specified. The gaseous product from the reactor was led to a terminator, where the remaining ozone was absorbed by KI solution. Both the electrolysis and E-peroxone processes were conducted under galvanostatic conditions using a DC power supply (DJS-292, Leici Co., Shanghai, China). The anode was a 6cm^2 plate (2cm*3cm) made of Pt, while the cathode was a 48cm^2 (6cm*8cm) activated carbon fiber electrode. The supporting electrolyte was Na_2SO_4 solution 0.05M. The electrolysis only process was initiated by turning on the DC power supply while the ozone generator was off. So-called E-peroxone process meant the DC power supply was turned on after the ozone generator was swithed on for 15 min to reach an almost steady ozone concentration. The mixture of O_2 and O_3 from the ozone generator, was bubbled into the reactor at 0.4 L•min-1, which is the same flow rate as in ozonation process. The ozonation, electrolysis, and E-peroxone process were run for 60 min. The runs were carried out at pH 3, 5, 7, 9 and 11, ozone dose was 3 g•h^{-1} and applied current density was 400mA unless otherwise specified. During ozonation, electrolysis, and E-peroxone process of AMO treatment, an aliquot of solution sample was collected from the reactor at various time intervals. Each run in the research was performed twice to ensure reproducibility.

Analytical Methods

The concentration of AMO was determined by HPLC (Waters, C18, λ=254nm). The mobile phase was a mixture of acetonitrile and 0.1% acetic acid with the volume ratio 5:95. A 10μL volume was injected using the auto sampler. TOC was measured using a TOC-VCPH analyzer (Shimadzu Co. Japan) to evaluate the mineralization of AMO during the treatment process.

The concentration of O_3 in solution was measured using the indigo method [26]. The •OH concentration was analyzed using a terephthalic acid (TA) trapping protocol. Briefly, the initial concentrations of TA (2 mM) and NaOH (5 mM) were added into the electrolyte in the reactor before the E-peroxone process started. And then the E-peroxone system was turned on, to generate •OH in the electrolyte. The •OH generated continuously during the E-peroxone process, then was trapped by the TA which is non-fluorescent, to form HTA which is highly fluorescent. The HTA concentration was determined using a fluorescence spectrophotometer (Hitachi, F-7000), which can be taken as a cumulative measurement of the •OH produced during the operation time [27, 28].

The intermediates of AMO degradation were measured by UPLC-MS/MS system, which consisted of a Waters ACQUITY UPLC instrument coupled to a TQD triple-quadrupole mass spectrometer (Waters Corp., Milford, MA). Separations were performed on an ACQUITY UPLC BEH C18 column (100 mm×2.1 mm) with a 1.7μm particle size equipped with a 0.2 μm pre-column filter unit and a guard column (Waters Corp.). The flow rate was set at 0.1 mL•min^{-1}. The column and autosampler tray temperature were both set at 40°C. The MS/MS instrument was operated with a capillary voltage of 1.00 kV, a source temperature of 350 °C and desolvation gas (nitrogen) at 350 °C with a flow of 900 L•h^{-1}. The interchannel delay was 20 ms. Parent and daughter ions, cone voltage and collision energy were optimized by automatic infusion of 1 mg•L^{-1} in a mixture of 50/50 water/acetonitrile containing 0.1% formic acid. Analysis was measured in positive electrospray ionisation (ESI+) mode; the mobile phase consisted of a mixture of solution A (0.1% formic acid in water) and solution B (0.1% formic acid in acetonitrile) with an initial composition of 90% solution A and 10% solution B. The mobile phase composition changed linearly from 10% solution B to 40% at 10.0 min, then solution B was re-equilibrated to starting conditions in 0.5 min and maintained for 1.5min [29].

Results and Discussion

Comparison of different process for AMO removal

Only 37% AMO was removed after 6 min treatment by electrolysis. While, AMO was completely degraded within 5 min and 4 min by ozonation process and E-peroxone process, respectively (Fig.1.a). The E-peroxone process enhanced the degradation rate of AMO comparing to the other two individual processes. The low removal rate of AMO in electrolysis resulted from the limited mass transfer rate of AMO molecules to the anode surface and the limited oxidation capacity of H_2O_2 [19, 30-32]. The ozonation process degraded the AMO slower than E-peroxone, indicating that O_3 utilization and •OH production were somewhat different in ozonation and E-peroxone process and influenced the degradation rate.

In addition, mineralization of AMO by different process was also evaluated in this work. Only 3.1% and 47.3% TOC mineralization was achieved after 60 min in electrolysis and ozonation process, respectively (Fig.1.b). When combined these two techniques (ozonation and electrolysis) together, so-called E-peroxone process, more than 67.8% TOC was removed in the same reaction time (Fig.1.b). Similarly with AMO degradation, low mineralization in electrolysis alone process resulted from the mass transfer limitation of AMO molecules to the anode surface as described for the low

degradation degree [19, 30]. As for ozonation, although O_3 could completely destruct the AMO structure in 5 min, it reacted rarely with the aliphatic carboxylic acids formed from the oxidation intermediates [33, 34]. In the long time mineralization of AMO, the •OH production in E-peroxone seemed to play an important role.

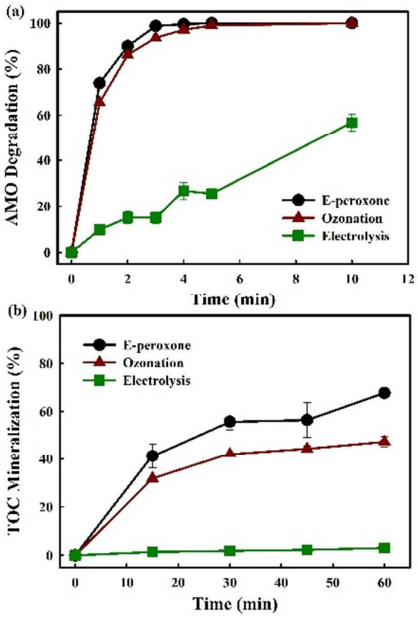

Fig.1 Degradation of AMO wastewater and TOC mineralization by electrolysis, ozonation and E-peroxone treatment (current of 400 mA; inlet O_3 concentration of 4 g•h^{-1})

It was shown that E-peroxone process provided a feasible and promising way to remove such kind of antibiotics and their intermediate products. However, how electricity introduction enhanced the O_3 utilization and •OH production in ozonation process for AMO treatment deserved further research.

•OH production and aqueous O_3 concentration in E-peroxone process

To understand the mechanism and evaluate the effect of electricity introduction in E-peroxone process, aqueous O_3 concentration and •OH production were compared in these two processes. The measurement of •OH production in the solution was through HTA production, which was the product by "•OH and TA" reaction.

Fig. 2 showed that when pure O_2 was sparged into the reactor during electrolysis (while the ozone generator was off), the H_2O_2 concentration increased almost linearly with reaction time. The result indicated that H_2O_2 was continuously produced from the sparged O_2 at the ACF cathode, which was consistent with Eq. (1). Conversely, when the ozone generator was turned on, the O_2 and O_3 gas mixture was sparged into the reactor, no H_2O_2 accumulation was observed.

In E-peroxone process, the concentration of HTA increased significantly within the first 8 min (Fig.2). The result indicated that in E-peroxone process the sparged O_3 and in-situ generated H_2O_2 reacted actively to continuously produce •OH (Eq. (2)), and then the produced •OH and TA formed HTA. After 8 min reaction time, HTA concentration decreased, since most TA had reacted with •OH, and then •OH and O_3 would consume HTA gradually [28]. In contrast, HTA was substantially low throughout the whole ozonation process. These results demonstrated that dissolved O_3 was consumed in the reaction with electro-generated H_2O_2 and electrochemical reactions such as cathode reduction to •OH in the E-peroxone process [17, 24]. As a result, •OH production was significantly enhanced in E-peroxone process, which contributed to higher AMO degradation rate in E-peroxone comparing to in ozonation process.

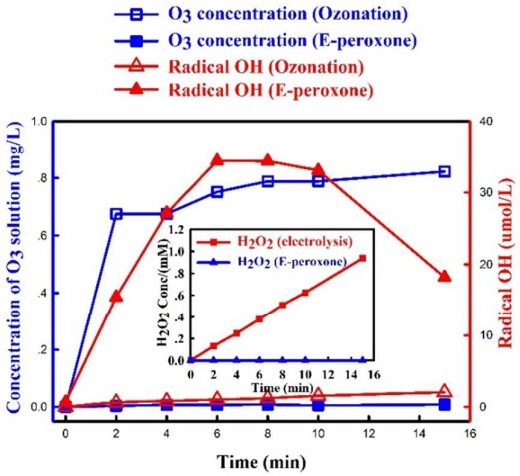

Fig. 2 Concentration of O_3 solution and radical OH during ozonation, and E-peroxone process and H_2O_2 concentration during electrolysis and E-peroxone in ionized water (current of 400 mA; inlet O_3 concentration of 4 g•h^{-1})

$$O_2 + 2H^+ + 2e^- \rightarrow H_2O_2 \quad (1)$$

$$O_3 + H_2O_2 + e^- \rightarrow \bullet OH + O_2 + \bullet OH^- \quad (2)$$

In ozonation process, the aqueous phase O_3 concentration increased rapidly to a plateau at ~0.8 mg•L^{-1}. In comparison, the aqueous O_3 concentration was substantially low during the whole E-peroxone treatment. These results indicated that dissolved O_3 was rapidly consumed in E-peroxone process. According to mass transfer theories [35], these electrochemically-driven reactions would enhance O_3 mass transfer from the gas phase to the liquid phase.

Consequently, the effective ozone dose would be higher in E-peroxone process than in ozonation. In other word, more sparged O_3 was transferred to the liquid phase for pollutants degradation in E-peroxone process rather than running out into gas phase in ozonation process.

The above results showed that in E-peroxone process, considerable amounts of •OH could be produced, and higher utilization rate of O3 was obtained as well. Therefore, it could be a reasonable interpretation for E-peroxone process performed more effective and economical than ozonation process for AMO degradation.

Effects of operating parameters on AMO degradation and TOC mineralization in E-peroxone

In order to control the E-peroxone treatment of Amoxicillin process efficiently and economically, important operating parameters such as O_3 concentration, current, and solution pH on the process performance were evaluated systematically.

Fig. 3 showed that increasing the O_3 concentration in the sparged gas enhanced both amoxicillin degradation and TOC mineralization in the E-peroxone process. This result can be easily rationalized because increasing the gas phase O_3 concentration would enhance the mass transfer of O_3 from gas phase to liquid

phase, which leads to higher •OH production rates from the reaction of aqueous O_3 with the in situ generated H_2O_2 in the solution. Consequently, amoxicillin and its degradation intermediates can be more rapidly mineralized as the gas phase O_3 concentration is increased.

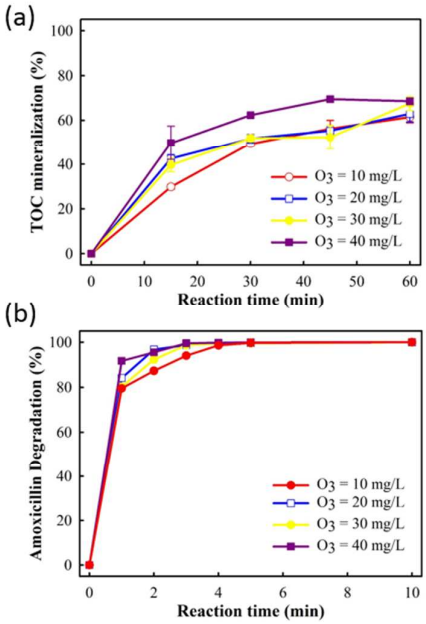

Fig.3 Effects of O_3 concentration on AMO degradation and TOC mineralization in E-peroxone process (current of 400 mA)

Fig. 4 showed that amoxicillin degradation and TOC mineralization increased as the applied current increased from 100 to 300 mA. However, further increasing the current to 400 mA did not enhance amoxicillin degradation and TOC mineralization accordingly. Consequently, increasing the applied current can produce more aqueous •OH when sufficient aqueous O_3 is available to react with the electro-generated H_2O_2, leading to enhanced pollutant degradation by the E-peroxone process. However, due to the low solubility of O_3, the •OH production rate would eventually be limited by the rate of O_3 transfer from gas phase to liquid phase when the current is increased beyond a critical value. When the amount of aqueous O_3 is insufficient in the solution, the excess H_2O_2 will contribute little to TOC mineralization because it is not a powerful oxidant. Therefore, the increasing the current beyond 300 mA did not increase the rate of amoxicillin degradation and TOC mineralization further, in the E-peroxone process.

In traditional ozonation treatment, pH is an important parameter, as ozone oxidation pathways include direct oxidation by molecular ozone under acidic conditions while indirect oxidation by •OH under alkaline pH values. However, how pH affected oxidation type and AMO structure present in E-peroxone process were both unclear. In the present study, effects of pH on AMO treatment in E-peroxone process were designed to clarify.

pH is usually considered as an important parameter for hydroxide ions initiate ozone decomposition, which involves the following reactions [36]:

$$O_3+OH^- \rightarrow HO_2^- + O_2;\ k = 70 M^{-1}s^{-1}; \quad (3)$$

$$O_3 + HO_2^- \rightarrow \bullet OH + O_2^- + O_2;\ k = 2.8*10^6\ M^{-1}s^{-1}; \quad (4)$$

$$HO_2^- + \bullet OH \rightarrow \bullet O_2H + \bullet OH^-; \quad (5)$$

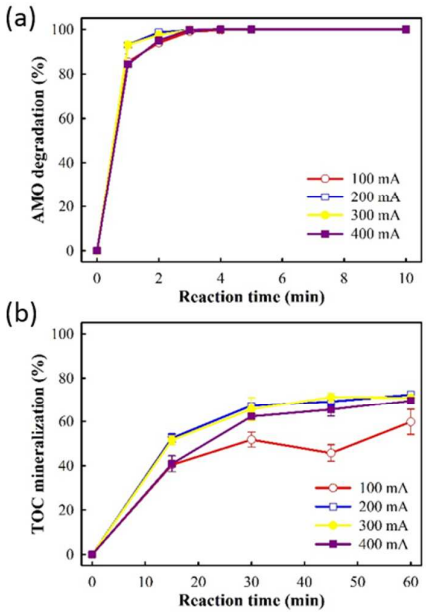

Fig.4 Effects of current on AMO degradation and TOC mineralization in E-peroxone process (inlet O3 concentration of 4g•h^{-1})

In E-peroxone process, when pH value was lower than 7.0, AMO degradation and TOC mineralization rate increased with pH (Fig.5.a and Fig.5.b). However, the enhancement effect of pH on AMO removal was limited when its value exceeded 7.0, and the highest removal rate was obtained at pH = 9, while the degradation and TOC mineralization rates of AMO decreased considerably when pH= 11. The result indicated that the effect of pH on AMO degradation was complicated and it varied at different solution pHs. For better understanding, the mechanism of these limited factors were discussed in detail.

Under acidic condition, the dissociation of H_2O_2 to HO_2^- would increase with pH. Further, H_2O_2 reacted with O_3 only when present as the anion, HO_2^-. The increase of H_2O_2 thus enhanced •OH generation in E-peroxone process via Eq. (4). This reaction well explained why AMO degradation and TOC mineralization rate went faster with the increase of pH.

Under alkali condition, it was accepted that aqueous ozone decomposing to HO_2^- (Eq. (3)) could enhance •OH generation in conventional ozonation process[36]. However, it might occur a side reaction and decrease the degradation efficiency when pH was at 11 in this study. It was shown that the availability of aqueous O_3 was substantially low when the E-peroxone process was conducted at 400 mA and neutral pH (Fig. 5). Increasing pH to 11 had further decreased the availability of aqueous O_3, due to the decomposition of O_3, causing the decrease in •OH production (Eq. (4)). Meanwhile, the dissociation of H_2O_2 would be enhanced with pH increase in E-peroxone process, as the pK_a of H_2O_2 was 11.6 at which favoured the production of excessive HO_2^- and further acted as a scavenger of •OH via Eq. (5). These reactions may account for the decrease in AMO degradation efficiency and lower TOC mineralization in E-peroxone process when E-peroxone (400 mA) was conducted at pH 11 than pH 7.

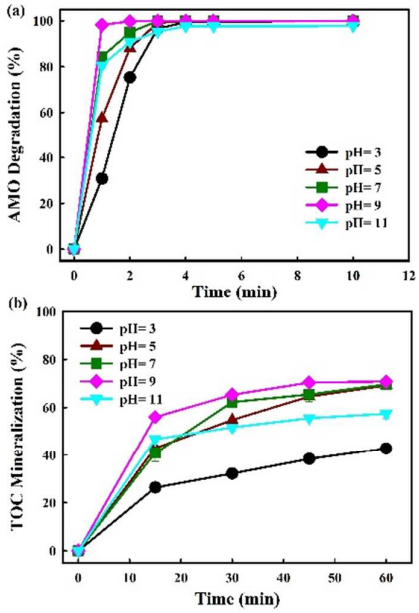

Fig.5 Effects of initial pH on AMO degradation and TOC mineralization in E-peroxone process (current of 400 mA; inlet O3 concentration of 4g•h^{-1})

The solution pH not only affected the decomposition of aqueous O3, but also influenced the existing forms of AMO, which affected AMO degradation efficiency in turn. AMO has three pK_a values of 2.68, 7.49 and 9.63 resulting in protonated, non-protonated and deprotonated forms, which could influence its degradation efficiency [37]. Considering the structure of the AMO, the pK_{a1} value of AMO carboxylic group is 2.68, and the protonation of carboxylic group formed at pH 2.6. Decreasing solution pH from 7 to 2.6 enhanced protonation of carboxylic acid products formed from AMO degradation. The protonation of AMO and carboxylic intermediates would generally decrease their susceptibility to •OH oxidation [38]. This could explain why E-peroxone process was more effective when it was operated at pH 7 than at pH 2.6, for AMO degradation and TOC mineralization. These results above showed that pH played an important role in AMO degradation, and pH controlled at 7 to 9 could guarantee hydroxyl radical production and AMO susceptibility to •OH oxidation in E-peroxone process.

Intermediates and AMO degradation pathway by ozonation and E-peroxone process

Although it seemed that E-peroxone process and ozonation had achieved similar removal effects on AMO, E-peroxone process had its own priority in AMO mineralization. Thus, it was assumed that the electricity influenced the AMO degradation on the intermediates species and pathways.

To investigate the influence of electricity on AMO degradation, the intermediates were identified precisely by UPLC-ESI-MS-MS. The degradation by-products were determined for AMO by ozonation and E-peroxone process corresponding with the different treatment process at starting pH of 6.0. 10 intermediates were detected in ozone process, while 15 intermediates were detected in E-peroxone process (Table 1). The main fragments observed in the mass spectra of each intermediate are indicated on Fig. 6 and Fig. 7.

Table 1. Accurate mass measurements found by UPLC-MS/MS spectra of AMO degradation fragmentation ions by ozonation and E-peroxone process.

Compound (m/z)	Structure	ozonation	E-peroxone
139	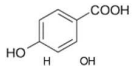	D	D
160		ND	D
176		D	D
231		ND	D
239	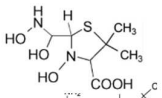	ND	D
310	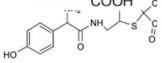	ND	D
340	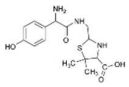	ND	D
354	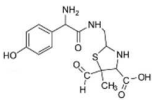	D	D
377	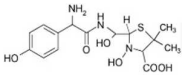	ND	D
382	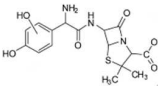	D	D
383	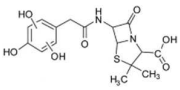	D	D
384	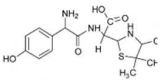	D	D
398	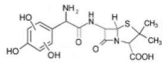	D	D
400	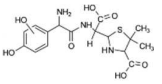	D	D
412	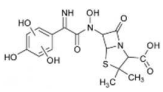	D	D
428	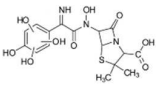	D	D

D= detected fragmentation, ND= not detected fragementation

Ozonation-based degradation pathway. The structure analysis of amoxicillin indicated that the ozone electrophilic attack occurred at the phenolic ring, sulfur atom, amino group and double bond. Based on this presumption, the following reaction pathways for AMO degradation by ozonation were proposed (Fig.6). The first one (Fig.6.A1, A2) was hydroxylation occurring in the phenolic ring and amino group, yielding the intermediates (m/z=382,383, 412,428)[13, 39]. Another pathway (Fig.6.B) was initialized by the attack of ozone on sulfur atom of amoxicillin, resulting into the formation and hydroxylation of the sulfoxide derivatives (m/z=382) and successively forming more complex compound (m/z=398,412,428) [39]. Pathway C began with the destruction of the four-membered β-lactam ring and
yields the penicilloic acid (m/z=384). A further decarboxylation the thiazolidine ring yielded the intermediates m/z=354. The pathway D was cleaved initially with the release of p-hydroxybenzoic acid (m/z = 139) by the ozone attack on double bond [40].

The bond cleavage generated at compounds (m/z=383, 412, 428) and further degradation losing the CO group and the four-membered β-lactam ring was evidenced compound m/z=176.

E-peroxone-based degradation pathway. Judging from the identified by-products, the following reaction pathways for AMO further degradation were proposed. The first one was hydroxylation, which could occur at the positions with lone pair of electrons including the benzoic ring (Fig.7.A1) and the nitrogen atom (Fig.7.A2). The pathway A1 and pathway A2 underwent the hydroxylation that one (m/z=382) to four hydroxyl groups (m/z=428) were added to the AMO molecule, yielding the intermediates with m/z=382, 383, 398, 412, 428 [39].

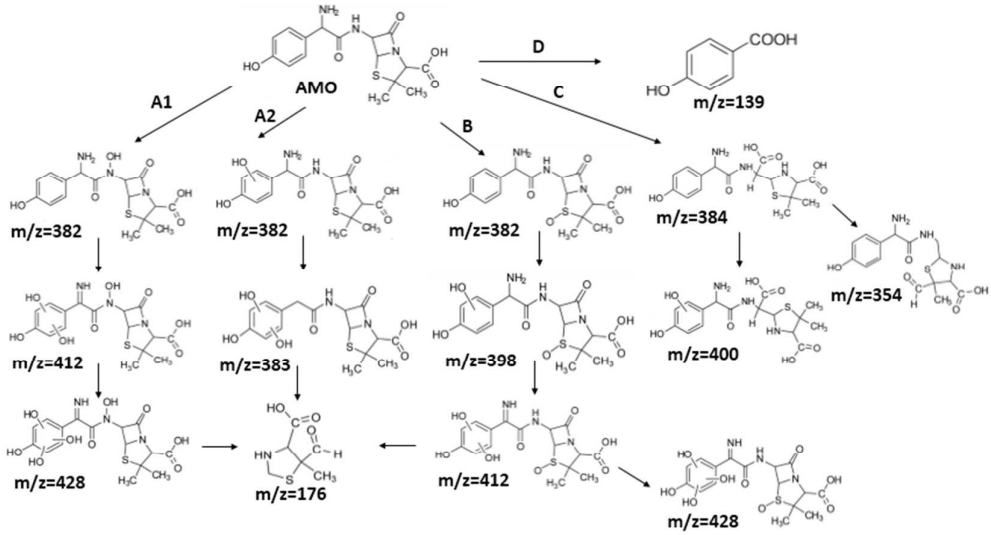

Fig.6 Proposed degradation pathway of AMO by Ozonation.

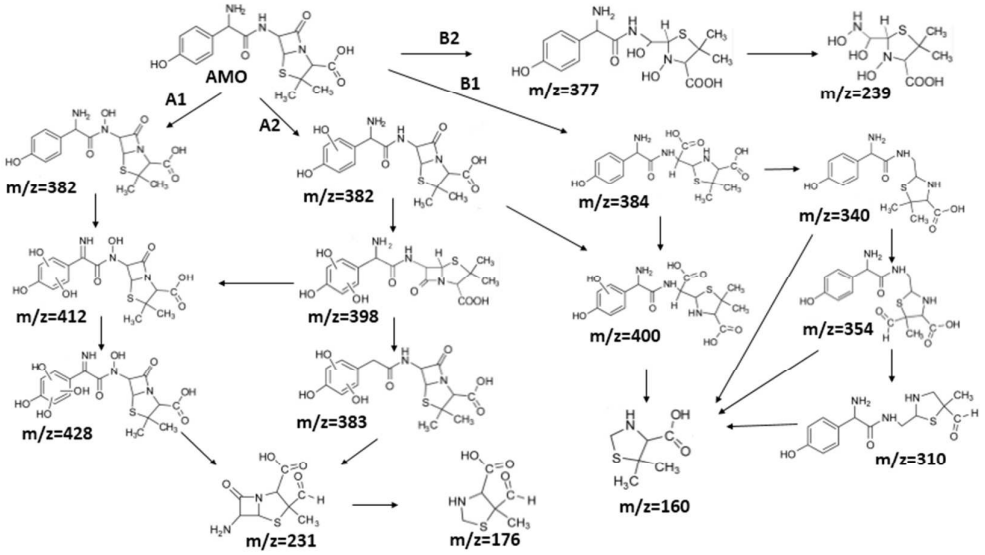

Fig.7 Proposed degradation pathway of AMO by E-peroxone.

Another degradation pathway (Fig.7.B1) corresponded to the opening of the four-membered β-lactam ring and yielded the penicilloic acid (m/z=384) and a series of derivatives (m/z=340,354,310,400). A further decarboxylation reaction yielded the intermediates m/z=340. The oxidation of the methyl groups in the thiazolidine ring was evidenced by the identification of the intermediates m/z=354 and m/z=310. The product with m/z = 160 could be also generated by the cleavage of the former derivatives[13]. The other pathway (Fig.7.B2) began with the destruction of lactamic bond yielding the intermediates (m/z=377) with its subsequent degradation to a product with m/z=239 [40].

The bond cleavage between nitrogen of the amino group and the carbonyl group was evidenced by compound m/z=231 and further degradation, due to the loss of the CO group and of the four-membered β-lactam ring, yielding the intermediates m/z=176.

It was found the introduction of electrolysis in ozonation had enhanced the cleavage of AMO, and then degraded to smaller products, so that AMO became easier to be attacked. Consequently, the removal rate of TOC was increased in E-peroxone process, comparing to ozone-alone process.

Conclusions

High removal efficiency and mineralization rate was obtained by E-peroxone over ozonation and electrolysis synergistic effect for amoxicillin treatment, owing to more effective hydroxyl radical production introduced by E-peroxone process. AMO was completely degraded in 4 min, and 67.8% total organic carbon (TOC) mineralization was obtained after 60 min by E-peroxone proecess. It was found that pH played an important role in AMO degradation and TOC mineralization, which not only affecting the decomposition of aqueous O_3 and the hydroxyl radical production, but also affecting the existing forms of AMO. The highest removal rates were obtained at pH= 9, indicating pH control was crucial in E-peroxone process.

The degradation pathways were deduced in two processes, based on the reaction between AMO and O_3 or •OH. 15 intermediates were identified in E-peroxone process while 10 intermediates were detected in ozone process using UPLC-MS/MS. These intermediates were generated in the following steps, the hydroxylation of the benzoic ring and N, the four-membered β-lactamic ring opening, oxidation of S, and other bond cleavage reactions. The introduction of electrolysis in ozonation had improved AMO degradation and increased TOC removal, suggesting E-peroxone process is feasible and has great potential for enhancing AMO treatment.

Acknowledgements

This work was financially supported by National Nature Science Foundation of China (51121062). The authors also gratefully acknowledge the financial support by State Key Laboratory of Urban Water Resource and Environment (2014TS06), National science and technology plan of China (2014BAD02B03), and Fund for young top-notch talent teachers by Harbin Institute of Technology (AUGA5710052514).

Notes and references

1. L.-H. Yang, G.-G. Ying, H.-C. Su, J. L. Stauber, M. S. Adams and M. T. Binet, *Environmental Toxicology and Chemistry*, 2008, **27**, 1201-1208.
2. S. K. Khetan and T. J. Collins, *Chemical Reviews*, 2007, **107**, 2319-2364.
3. J.-P. Besse and J. Garric, *Toxicology Letters*, 2008, **176**, 104-123.
4. F. Pomati, S. Castiglioni, E. Zuccato, R. Fanelli, D. Vigetti, C. Rossetti and D. Calamari, *Environmental Science & Technology*, 2006, **40**, 2442-2447.
5. K. Kuemmerer, *Chemosphere*, 2009, **75**, 417-434.
6. K. Kuemmerer, *Chemosphere*, 2009, **75**, 435-441.
7. P. Verlicchi, M. Al Aukidy and E. Zambello, *Science of the Total Environment*, 2012, **429**, 123-155.
8. H. W. Leung, T. B. Minh, M. B. Murphy, J. C. W. Lam, M. K. So, M. Martin, P. K. S. Lam and B. J. Richardson, *Environment international*, 2012, **42**, 1-9.
9. B. Kasprzyk-Hordern, R. M. Dinsdale and A. J. Guwy, *Water Research*, 2008, **42**, 3498-3518.
10. S. Castiglioni, R. Bagnati, R. Fanelli, F. Pomati, D. Calamari and E. Zuccato, *Environmental Science & Technology*, 2006, **40**, 357-363.
11. K. Ikehata, N. J. Naghashkar and M. G. Ei-Din, *Ozone-Science & Engineering*, 2006, **28**, 353-414.
12. H. Stockinger, E. Heinzle and O. M. Kut, *Environmental Science & Technology*, 1995, **29**, 2016-2022.
13. R. Andreozzi, M. Canterino, R. Marotta and N. Paxeus, *J Hazard Mater*, 2005, **122**, 243-250.
14. I. A. Balcioglu and M. Otker, *Chemosphere*, 2003, **50**, 85-95.
15. R. F. Dantas, S. Contreras, C. Sans and S. Esplugas, *Journal of Hazardous Materials*, 2008, **150**, 790-794.
16. J. Staehelin and J. Hoigne, *Environmental Science & Technology*, 1982, **16**, 676-681.
17. S. Yuan, Z. Li and Y. Wang, *Electrochemistry Communications*, 2013, **29**, 48-51.
18. J. Pablo Pocostales, M. M. Sein, W. Knolle, C. von Sonntag and T. C. Schmidt, *Environmental Science & Technology*, 2010, **44**, 8248-8253.
19. C. A. Martinez-Huitle and E. Brillas, *Applied Catalysis B-Environmental*, 2009, **87**, 105-145.
20. A. Xu, X. Li, S. Ye, G. Yin and Q. Zeng, *Applied Catalysis B-Environmental*, 2011, **102**, 37-43.
21. R. G. Rice, *Ozone-Science & Engineering*, 1997, **18**, 477-515.
22. I. Arslan-Alaton and A. E. Caglayan, *Ecotoxicology and Environmental Safety*, 2006, **63**, 131-140.
23. B. De Witte, J. Dewulf, K. Demeestere and H. Van Langenhove, *Journal of Hazardous Materials*, 2009, **161**, 701-708.
24. B. Bakheet, S. Yuan, Z. Li, H. Wang, J. Zuo, S. Komarneni and Y. Wang, *Water Res*, 2013, **47**, 6234-6243.
25. Z. Li, S. Yuan, C. Qiu, Y. Wang, X. Pan, J. Wang, C. Wang and J. Zuo, *Electrochimica Acta*, 2013, **102**, 174-182.

26. H. Bader and J. Hoigne, *Water Research*, 1981, **15**, 449-456.
27. N. Milan-Segovia, Y. Wang, F. S. Cannon, R. C. Voigt and J. C. Furness, Jr., *Ozone-Science & Engineering*, 2007, **29**, 461-471.
28. I. Hua and M. R. Hoffmann, *Environmental Science & Technology*, 1997, **31**, 2237-2243.
29. M. Carlier, V. Stove, J. A. Roberts, E. Van de Velde, J. J. De Waele and A. G. Verstraete, *International Journal of Antimicrobial Agents*, 2012, **40**, 416-422.
30. E. Brillas, I. Sires, C. Arias, P. L. Cabot, F. Centellas, R. M. Rodriguez and J. A. Garrido, *Chemosphere*, 2005, **58**, 399-406.
31. A. Oezcan, M. A. Oturan, N. Oturan and Y. Sahin, *Journal of Hazardous Materials*, 2009, **163**, 1213-1220.
32. J. Hastie, D. Bejan, M. Teutli-Leon and N. J. Bunce, *Industrial & Engineering Chemistry Research*, 2006, **45**, 4898-4904.
33. A. Lopez, H. Benbelkacem, J. S. Pic and H. Debellefontaine, *Environmental technology*, 2004, **25**, 311-321.
34. M. J. Quero-Pastor, M. C. Garrido-Perez, A. Acevedo and J. M. Quiroga, *Science of the Total Environment*, 2014, **466**, 957-964.
35. E. L. Cussler, *Diffusion: mass transfer in fluid systems*, Cambridge university press, 2009.
36. U. von Gunten, *Water Research*, 2003, **37**, 1443-1467.
37. A. F. Goddard, M. J. Jessa, D. A. Barrett, P. N. Shaw, J. P. Idstrom, C. Cederberg and R. C. Spiller, *Gastroenterology*, 1996, **111**, 358-367.
38. G. V. Buxton, C. L. Greenstock, W. P. Helman, A. B. Ross and W. Tsang, *Journal of Physical and Chemical Reference Data*, 1988, **17**, 513.
39. A. G. Trovo, R. F. P. Nogueira, A. Aguera, A. R. Fernandez-Alba and S. Malato, *Water Research*, 2011, **45**, 1394-1402.
40. D. Klauson, J. Babkina, K. Stepanova, M. Krichevskaya and S. Preis, *Catalysis Today*, 2010, **151**, 39-45.

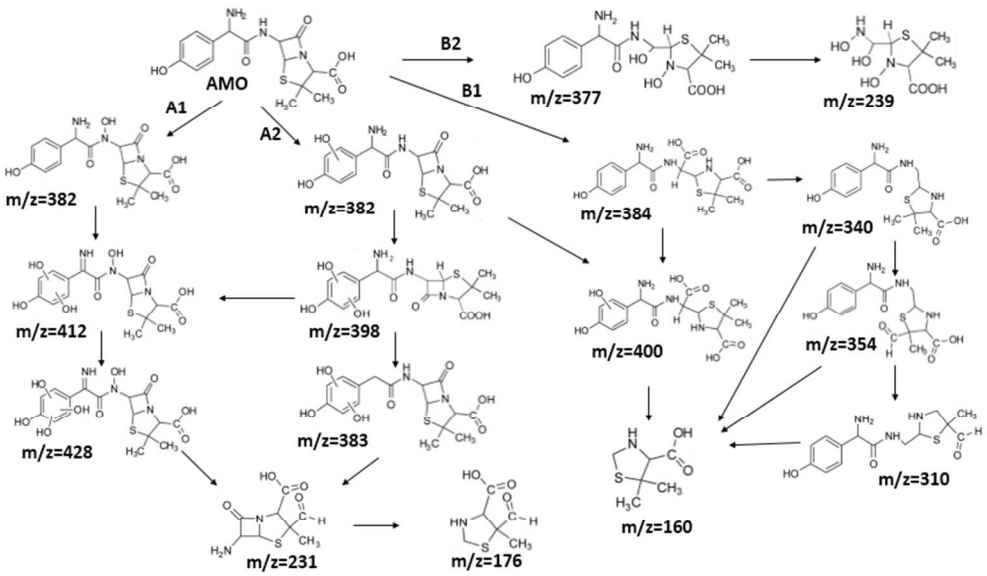

Proposed degradation pathway of AMX by E-peroxone

228x141mm (96 x 96 DPI)